Molecular docking studies of a phytocompound kanzonol B as a potential acetylcholine esterase inhibitor for epilepsy

Lim Joe SIANG¹ and Ravichandran VEERASAMY*2,3

¹Research Scholar, Faculty of Pharmacy, AIMST University, Semeling-08100, Bedong, Kedah, Malaysia ²Faculty of Pharmacy, AIMST University, Semeling-08100, Bedong, Kedah, Malaysia ³Saveetha Dental College and Hospitals, Saveetha Institute of Medical and Technical Sciences, Chennai, Tamil Nadu, India

Abstract. The third most prevalent neurological condition in the world is epilepsy. It has become a major concern for both medicine and public health in recent years. Currently, there are many approved therapies to address epilepsy diseases, but most of them are often associated with undesirable effects. Recent studies have pointed out the advantages of Acetylcholine Esterase Inhibitors (AChEIs) in the treatment of epilepsy with their ability to modulate cholinergic transmission and neuroprotective effects. However, AChEIs have adverse drug effects, necessitating the design of a novel drug. Flavonoids have emerged as promising alternatives in neuropharmacology due to their reported positive role in cognitive dysfunction, learning, and memory deficits. Thus, we aimed to identify the potential Acetylcholine Esterase (AChE) inhibitory activity of kanzonol B. The molecular docking simulation was used in the current in silico investigation to evaluate kanzonol B's capacity to bind with Torpedo californica AChE (TcAChE). Additionally, ADMET screening was performed on kanzonol B to forecast its pharmacokinetic characteristics. According to our findings, kanzonol B exhibited a considerable binding affinity (-10.58 kcal/mol) against the TcAChE enzyme. It also complied with the druglikeness characteristics and Lipinski's RO5. The standard drug donepezil had a binding affinity of -11.73 kcal/mol. But both donepezil and kanzonol B interacted with ARG289, PHE331, PHE288, TRP84, PHE330, ILE287, SER286, TYR334, GLY441, HIS440, and PHE290. According to these computer studies, kanzonol B may have a therapeutic use for epilepsy as a strong AChE enzyme inhibitor. Therefore, to confirm the encouraging findings of the current in silico work, we advise more experimental research.

Keywords: acetylcholine esterase; kanzonol B; molecular docking; pharmacokinetics; drug-likeness profiles; epilepsy.

1. Introduction

A serious neurological condition called epilepsy causes both recurrent and spontaneous seizures. Globally, it is the third-leading cause of neurological disease burden, affecting around 50 million people in the world [1]. About 30% of epileptic patients are not responding to the treatments and are suffering from the medications' associated side effects and interactions [2, 3]. To improve seizure control, it is necessary to create new antiepileptic medications (AEDs) with multitargeting and a tolerable profile [4]. The role of acetylcholinesterase (AChE) in epilepsy is a complex area due to its dual role in modulating cholinergic signaling and the brain's inflammatory response. A crucial neurotransmitter in the central cholinergic system is acetylcholine (ACh). ACh exerts antiinflammatory effects in the brain, primarily through muscarinic receptors, and it suppresses the microglial activation and the release of pro-inflammatory cytokines. However, following seizure activity, AChE is often upregulated, leading to a rapid decline in available ACh. This will diminish the cholinergic antiinflammatory response, increase the microglial activation, and increase the levels of pro-inflammatory

cytokine IL-1\beta. This heightened inflammatory state can promote neuronal hyperexcitability and epileptogenesis [5].

AChE inhibitors (AChEIs) have emerged as a promising approach to address the neurotransmitter imbalance and inflammatory response. Donepezil, a well-known AChE inhibitor approved for Alzheimer's disease (AD), demonstrates neuroprotective effects in an epilepsy model. A study has shown that donepezil administration for a period of three weeks after seizures subside significantly reduces neuronal death, oxidative stress, and microglial activation. The antiepileptic potential of donepezil is also demonstrated in a study that showed resistance to induced seizures was increased in a mouse model of Dravet syndrome [6]. These findings suggest that AChEIs administration might be useful for epilepsy [7].

Additionally, the central cholinergic system is also important in the memory processes. Degeneration or dysfunction of cholinergic neurons is often observed in aging individuals, particularly with cognitive decline and memory impairment. Similarly, studies in epileptic mice have shown a significant decrease in ACh levels, which may be linked to impaired memory performance [8]. This impairment occurs because epilepsy can

^{*} Corresponding author. *E-mail address*: ravichandran_v@aimst.edu.my (Ravichandran Veerasamy)

negatively impact cholinergic function in brain regions, particularly the hippocampus, which is crucial for memory. The increase in ACh availability has been demonstrated to improve the memory in epilepsytreated mice. Therefore, these findings support the potential use of AChEIs to modulate seizure activity and inflammation and also to alleviate epilepsy-associated cognitive deficits. However, AChEIs are often associated with adverse effects. such neuropsychiatric, gastrointestinal, and cardiovascular, due to the overstimulation of peripheral cholinergic activity and muscarinic receptor activation [9, 10]. Reports of AChEI-induced adverse drug reactions (ADRs) have increased over the last decades, with 70% being severe and up to 2.3% being fatal [11].

According to recent reports, huperzine A, an AChEI derived from lycopod plants [12], may have antiepileptic properties through enhancing GABAergic intracortical inhibition [13]. Furthermore, anticholinesterases, which have a higher seizure tolerance, can be utilized as an adjuvant therapy to treat epilepsy-related cognitive impairment [14]. Therefore, traditional anti-epileptic properties of medicinal plants may aid Alzheimer's patients who also have epilepsy, and they may also serve as a source of natural pharmaceuticals for neurological conditions.

Flavonoids, naturally occurring polyphenolic components found in fruits and vegetables, have attracted significant interest and attention due to their various beneficial effects on health, including antiinflammatory, antimicrobial, antioxidant, antimutagenic, and anticancer effects. [15]. Numerous in vitro and in vivo studies have been conducted to evaluate the antioxidant and neuroprotective properties of flavonoids. Numerous studies [16-18] have demonstrated and highlighted the role of flavonoids in preventing and treating cognitive dysfunction, learning, and memory deficits. Due to the potential beneficial effects of flavonoids on health, flavonoids may be considered as potential adjunct therapeutic agents for epilepsy and to improve cognitive function in epilepsy patients.

Kanzonol B is a prenylated flavonoid known from plants such as Dorstenia barteri, Glycyrrhiza eurycarpa, and Canarium odontophyllum [19-21]. It has been recently reported that kanzonol B can be a potential chelator in the treatment of neuroinflammatory disorders by downregulating iNOS and COX-2 in activated microglial cells [22]. Based on these findings, we aimed to determine the acetylcholinesterase (AChE) inhibiting activity of kanzonol B, which may be of value for patients with epilepsy or cognitive dysfunction. Compared to traditional methods of drug design, such as synthesis, in vitro and in vivo studies, computer-aided drug design can significantly shorten the development time due to the prediction of the pharmacokinetics, stability, and efficacy of a compound and thus save on time, cost, and manpower. Herein, we evaluated kanzonol B as an AChE inhibitor by molecular docking and assessed ADMET properties to estimate safety and potential efficacy. Donepezil was used as a reference drug, as it is a clinically approved AChE inhibitor with a clearly understood pharmacological profile. Kanzonol

B is compared to donepezil as a good reference for its binding efficacy and therapeutic potential, which assures the relevance of the study and its applicability to clinical practice.

2. Computational details

2.1. Molecular docking studies

The structures of the enzyme and kanzonol B were obtained from online databases, such as the Protein Data (https://www.rcsb.org/) Bank and PubChem (https://pubchem.ncbi.nlm.nih.gov/). Additionally, the modeling software such as Chem Office-16 (https://chemistrydocs.com/chemoffice-2016chemdraw-professional-2016/), Discovery Visualizer 2020 (https://discover.3ds.com/discoverystudio-visualizer-download), AutoDock 4.2.6 and AutoDock Too1 1.5.7 (https://ccsb.scripps.edu/mgltools/downloads/), Swiss-PdbViewer (https://spdbv.unil.ch/) and PyMOL Win (https://www.pymol.org/), online tool SwissADME (http://www.swissadme.ch/), SAVES 6.0 (https://saves. mbi.ucla.edu/), **ProSA** (https://prosa.services. came.sbg.ac.at/prosa.php), ProO (https://prog.bioinfo.se/ProO/ProO.html). **ProTox** (https://tox-new.charite.de/ protox II/), toxCSM (https://biosig.lab.uq.edu.au/toxcsm/), and UCSF-Chimera (https://www.cgl. ucsf.edu/chimera/) were used in the present study.

2.2. Processing of ligands for docking

Kanzonol B's structure was obtained as a.sdf file from PubChem (Figure 1). Additionally, PubChem provided the structure of donepezil, the common FDA-approved AChEI medication. Then, using MM2 force field techniques, both structures were transformed into 3D structures and put through an energy reduction process in Chem Office-16's Chem3D tool. Hydrogens and charges were added to each structure before it was saved as a.sdf file for subsequent use.

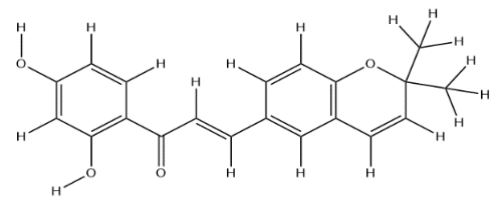


Figure 1. Structure of kanzonol B

2.3. Processing of enzyme for docking

The researchers obtained the three-dimensional structure of the enzyme Torpedo californica AChE (TcAChE) (PDB ID: 5NAU) from the PDB for this investigation. This enzyme has a resolution of less than 3 Å and is not mutated. The crystallographic structure was inspected for defects and broken chains using PyMOL. PyMOL was used to add the missing residues at the end of the enzyme chains. The restored enzyme was then verified after being energy reduced in UCSF-Chimera using the SWISS-PDB viewing tool.

2.4. Modeled enzyme quality assessment

To assess the prepared enzyme structure, SAVES v 6.0 was utilized. SAVE version 6.0 was used to upload the enzyme structure in PDB format, and the pertinent

parameters were assessed. Model quality was evaluated using ERRAT, Verify3D, and PROCHECK. The modeled structure with the superior result was chosen for further studies [23].

2.5. Active sites determination

The active site of the enzyme was identified with the help of Discovery Studio Visualizer 2020.

2.6. Docking protocol validation

The redocking technique was used to validate the docking methodology. Using AutoDock 4.2.6, the ligand's crystallographic structure of the ligand from the protein complex was re-docked against the same enzyme. Next, PyMOL was used to calculate the RMSD of the re-docked ligand against its initial crystallographic structure [24].

2.7. Molecular docking studies

Docking investigations were conducted using the AutoDock tool 1.5.7 (AutoDock 4.2.6). Water, Kollman charges, and polar hydrogens were eliminated to prepare the protein. The ligands were protonated, and then Gasteiger charges were added. Following that, the ".pdbqt" format was used to save both the ligands and the enzyme. The active Grid box was transformed by typing the X, Y, and Z values of coordinates obtained using Discovery Studio Visualizer [25]. All the docking parameters were kept as default values, except the population size (300), number of genetic algorithm (GA) trials (50), and maximum number of evaluations (long). After the docking studies using the Lamarckian Genetic Algorithm, and based on the binding affinity, the best conformer was selected. The docking output files were then analyzed for drug-amino acid residue interactions in the enzyme using Discovery Studio Visualizer 2020. A 2D protein-ligand binding interaction map and the resulting 3D docking pose were generated and used for further discussion of ligandtarget binding interactions [26].

2.8. Drug likeness and ADMET studies

The Chem3D program was used to determine kanzonol B's SMILES code. The BBB and CNS permeabilities were calculated using the PreADMET software, and the ADME properties of kanzonol B were ascertained using SwissADME [27, 28]. Lipinski's and Veber's rules were used to forecast how drug-like kanzonol B would be. The ProTox and toxCSM servers were also used to evaluate Kanzonol B's toxicity. The toxCSM service predicts numerous important toxicity factors, including nuclear responses, stress responses, genomic, environmental, dose-response, and organic responses [29]. SwissADME predicted drug likeness and ADMET results of kanzonol B were already reported elsewhere [Reproduced from Ref. 21].

3. Results and discussion

3.1. Molecular docking studies

3.1.1. Modelled enzyme. A few residues were absent from the head and tail sections of TcAChE (PDB ID: 5NAU), which was obtained from the PDB. Therefore,

the PyMOL molecular viewer was used to model it by adding the missing residues. Next, it was done by aligning the restored enzyme structure with the original structure. The alignment of the genuine enzyme (green) and the modeled enzyme (blue) is shown in Figure 2. Since the RMSD was less than 2 Å, the RMSD for these structures was determined to be 0.205 (4205 to 4205 atoms), suggesting a high similarity between these enzymes.

3.1.2. Modelled enzyme validation. Model quality was evaluated using protein structure verification services like ProSA-web and SAVES 6.0. Tables 1 and 2 demonstrate that more than 90% of the amino acid residues were located in the most favored and extra-allowed regions, which demonstrates the high quality, stability, and dependability of the model. Additionally, strong model quality is indicated by a G-factor of > -0.5 overall (Table 3) [30-32].

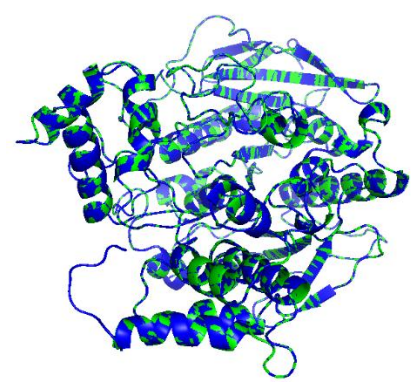


Figure 2. Alignment of the original TcAChE (5NAU) and modelled enzyme structure

By examining the statistics of non-bonded interactions between various atom types, ERRAT assesses the quality of models; higher scores denote higher quality [33]. This parameter represents a good high-resolution model with a score of 95% or above [32]. Nonetheless, it is widely acknowledged that a model of high quality has a quality factor of greater than 50% [34, 35]. The modeled acetylcholinesterase's ERRAT value above 95% in the current investigation indicated high resolution. A model Z-score within the range indicates a high-quality model, whereas a score that is outside the range indicates structural inaccuracy [36]. According to Tables 1 and 2, the modeled enzyme's scores were within the range of native proteins of comparable sizes.

This enzyme model's dependability is further supported by the local model quality estimation, which shows a lower energy than zero for the modeled enzyme. ProQ, which was also used to assess the quality of the enzyme structure, predicted LG score of the modeled enzyme was greater than 6, indicating that the modeled protein is extraordinarily good [34]. Furthermore, the modeled enzyme's Verify3D values revealed that the model passes the criteria with high scores (> 80%). The modeled enzyme's overall high quality and appropriateness for the molecular docking studies were confirmed when it fulfilled the validation criteria.

Table 1. Ramachandran plot, z-score, and local model quality of the modelled enzyme

Table 2. Validation metrics of the modelled enzyme

Protein PBD ID	Validation Metric	
Modelled 5NAU	ERRAT (%)	95.6685
	Overall quality factor	93.0083
	Verify 3D (%)	Pass
	Ramachandran plot (%)	
	Most favored	88.1%
	Additional allowed	11.4%
	Generously allowed	0.2%
	Disallowed	0.2%
	Overall G-factors	-0.15
	ProSA Z-Score	-10.58
	ProQ	
	Lgscore	6.390

3.1.3. Docking protocol validation. The RMSD was calculated by superimposing the top-ranked poses onto their co-crystallized pose (Table 3).

Table 3. Validation criteria for docking protocol

Protein	Crystal ligand name	RMSD (Å)
Modelled Torpedo californica acetylcholinesterase (TcAChE)	(2~{E})-5-methoxy-2- [[1- (phenylmethyl)piperidin- 4-yl]methylidene]- 3~{H}-inden-1-one	1.82

The RMSD value accurately predicts the ligand's shape, orientation, and position in relation to its reference native pose [37]. The ligand location is more closely aligned with the native ligand morphology when the RMSD value is lower. An RMSD value of less than 2 Å between docked and original crystallographic ligands suggests a valid docking methodology and acceptability for the docking operation [38]. However, an acceptable range for an RMSD is 2 Å to 3 Å. On the other hand, an RMSD greater than 3 Å is deemed unsatisfactory [39]. It is widely acknowledged that the most efficient criterion for verifying correctly posed

molecules is an RMSD cut-off value of less than 2 Å [40, 41].

Table 3 shows that the re-docked ligand binds similarly to the co-crystallized ligand in the enzyme's binding pocket, with an RMSD value of less than 2 Å. The resulting RMSD value attests to the successful validation of the docking methodology and its suitability for accurately and specifically docking the test chemical against the chosen enzyme.

3.1.4. Docking studies. Table 4 shows the binding affinities of kanzonol B and donepezil, the standard drug, to TcAChE. Figure 3 depicts two-dimensional interactions and binding interaction surface poses on receptors. Nonetheless, Table 5 showed the amino acid residues implicated in interactions.

Table 4. Docking scores of Kanzonol B and the standard drug

Protein	TcAChE
Compounds	Kanzonol B
Binding affinity (kcal/mol)	-10.58
Standard drugs	Donepezil
Binding affinity (kcal/mol)	-11.73

Table 5. Amino acid residues of proteins interacted with kanzonol B, a standard drug and crystallographic ligand

Enzyme PDB ID (used			Bound amino acid residues					
after adding missing residues)	Ligand	Hydrogen	Hydrophobic	van der Waals	Electrostatic	Others		
5NAU	Standard	ARG289,	PHE330,	TYR121,	HIS440	-		
	(Donepezil)	PHE288	TRP84, TRP84,	PHE290,				
			HIS440,	PHE331,				

Enzyme PDB ID (used		Bound amino acid residues				
after adding missing residues)	Ligand	Hydrogen	Hydrophobic	van der Waals	Electrostatic	Others
			LEU282,	SER286,		
			TRP279,	GLY335,		
			TYR334,	GLY441,		
			ILE287	GLU199		
5NAU	Kanzonol B	ARG289,	TRP84,	GLY335,	-	-
		ARG289,	PHE330,	SER286,		
		PHE331,	PHE331,	TYR334,		
		PHE288	ILE287	GLY118,		
				GLY441,		
				HIS440,		
				PHE290,		
				ILE288,		
				TRP279,		
				LEU282		
5NAU	Crystallographic	ARG289,	LEU282,	VAL71,	-	-
	ligand	PHE331,	TYR334,	SER122,		
	$((2\sim\{E\})-5$ -methoxy-	SER286,	ILE287	PRO86,		
	2-[[1-	ASP72,		ASN85,		
	(phenylmethyl)piperid	PHE288		TRP84.		
	in-4-yl]methylidene]-			PHE330,		
	$3\sim\{H\}$ -inden-1-one)			GLY335,		
				TRP279,		
				TYR70,		
				PHE290,		
				TYR121		

3.1.5. Binding to TcAChE (PDB ID: 5NAU). The main protein targets in antiepileptic drug discovery are focused on the GABA receptor, ion channels, and signaling proteins. In our previous works, we reported the molecular docking studies on the primary targets in epilepsy studies [21]. While these targets directly modulate seizure activity, other proteins are also often included in docking studies to assess potential secondary or supportive effects. AChE has been increasingly recognized as a valuable in silico docking target in epilepsy research. Beyond serving as a primary target in AD, AChE is also incorporated in docking studies for epilepsy research to assess whether the candidate antiepileptic compounds may affect the cholinergic balance, contributing to seizure regulation or cognitive effects.

For example, in the evaluation of olivetol as a potential anticonvulsant, AChE was selected alongside MAPK, Caspase-3, and histone deacetylase for molecular docking [42]. This has reflected AChE involvement in epilepsy pathways. Similarly, another study aimed to screen the novel carboxamide derivatives against both AChE and butyrylcholinesterase (BChE), in combination with in vivo anticonvulsant testing, assessing the dual role of the candidate compounds in modulating cholinergic signaling in addition to seizure control [43]. These studies have highlighted that AChE may serve as an auxiliary target in antiepileptic drug design. By docking compounds against AChE in epilepsy studies, it offers insights into the cholinergic pathway. Therefore, in this work, we incorporated TcAChE to explore the AChE inhibition potential of kanzonol B.

Kanzonol B demonstrated molecular interactions with a binding score of -10.58 kcal/mol on the TcAChE active site residue. While hydrophobic connections were

created at residues TRP84, PHE330, PHE331, and ILE287, kanzonol B generated four H-bond contacts with residue ARG289 using two bonds (1.88 Å and 2.24 Å), PHE331 (2.08 Å), and PHE288 (2.51 Å) of the TcAChE, as seen in Figure 3a. With a binding score of 11.73 kcal/mol, the conventional medication donepezil also displayed eight hydrophobic contacts at PHE330, TRP84 (two bonds), HIS440, LEU282, TRP279, TYR334, and ILE287 on the acetylcholinesterase enzyme, in addition to two H-bonds with ARG289 (2.27 Å) and PHE288 (2.77 Å) (Figure 3b).

Additionally, it experienced a single electrostatic contact at HIS440. In contrast to donepezil at TYR121, PHE290, PHE331, SER286, GLY335, GLY441, and GLU199, a small number of van der Waals interactions were detected between TcAChE and kanzonol B at GLY335, SER286, TYR334, GLY118, GLY441, HIS440, PHE290, ILE288, TRP279, and LEU282. Five H-bonds were seen with ARG289 (2.24 Å), PHE331 (2.79 Å), SER286 (3.04 Å), ASP72 (3.14 Å), and PHE288 (2.59 Å) in the crystallographic ligand interaction that was derived from the TcAChE model. The binding score of the interaction was -12.02 kcal/mol. Additionally, it exhibited three hydrophobic interactions at LEU282, TYR334, and ILE287 (Figure 3c).

In the context of our investigation, kanzonol B had a binding score of -10.58 kcal/mol, and its interaction profile included four hydrogen bonds with ARG289, with 2 bonds (1.88 Å and 2.24 Å), PHE331 (2.08 Å), and PHE288 (2.51 Å), and four hydrophobic interactions with TRP84, PHE330, PHE331, and ILE287. While donepezil had a binding score of -11.73 kcal/mol, and its interactions with the TcAChE active site were characterized by two H-bonds at ARG289 (2.27 Å) and PHE288 (2.77 Å), eight hydrophobic

interactions with PHE330, TRP84 (two bonds), HIS440, LEU282, TRP279, TYR334, and ILE287, and one electrostatic interaction at HIS440.

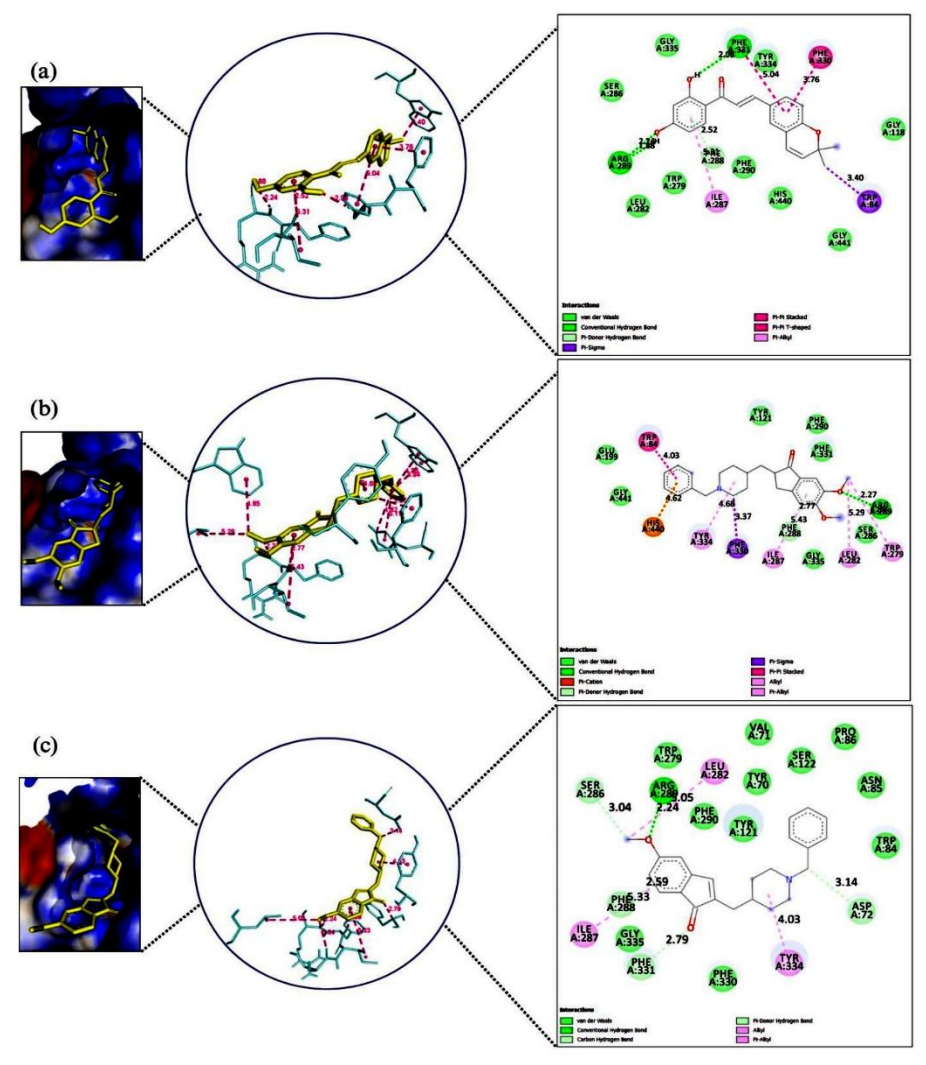


Figure 3. 2D Interaction map of TcAChE with (a) kanzonol B; (b) donepezil; (c) crystallographic ligand.

The crystallographic ligand demonstrated the strongest binding to the TcAChE, forming an extensive network of five hydrogen bonds. These included interactions at ARG289 (2.24 Å), PHE331 (2.79 Å), SER286 (3.04 Å), ASP72 (3.14 Å), and PHE288 (2.59 Å). Three hydrophobic contacts were also formed at LEU282, TYR334, and ILE287.

The oligomeric forms of AChE seen in electric fish, such as Electrophorus and Torpedo, share structural similarities with those found in humans [44]. The conserved catalytic mechanism of TcAChE with human AChE makes it a valid model for docking studies. Additionally, TcAChE has been extensively researched and utilized in multiple studies [44-46]. Thus, this enzyme was selected and used in our study. The roles of the amino acid residues PHE288, ARG289, and PHE331 of TcAChE in ligand binding for TcAChE inhibition have been highlighted in various studies [47]. AChE is a complex enzyme characterized by an alpha/beta hydrolase fold and an overall ellipsoid structure. It features a deep and narrow groove of 20 Å known as the aromatic gorge [48]. The precise geometry of the catalytic triad, which involved conserved residues SER

200, HIS400, and GLU327 within the active site gorge of AChE from *Torpedo californica*, had been demonstrated through the high-resolution structural analyses [49]. As we can observe from Figure 3a, kanzonol B interacted only with the key residue HIS 400 through van der Waals at the catalytic triad. In contrast, donepezil interacted with HIS440 through both hydrophobic and electrostatic interactions (Figure 3b). The crystallographic ligand did not show any contact with any catalytic triad residues (Figure 3c).

The three conserved residues that make up TcAChE, the peripheral anionic site (PAS)—TYR70, TYR121, and TRP279—restrict access to the gorge [50]. In our study, kanzonol B formed a van der Waals interaction with TRP279. On the other hand, donepezil established $\pi\text{-alkyl}$ interactions with TRP279 and van der Waals interactions with TYR121. The crystallographic ligand formed van der Waals interactions with all three PAS residues at the peripheral binding site.

Furthermore, the acyl pocket, which is a key determinant of ChE specificity in TcAChE, is characterized by PHE288 and PHE290 [51]. Our analysis revealed that PHE288 contributed to hydrogen

bonding with kanzonol B, donepezil, and the crystallographic ligand. Likewise, all three ligands showed evidence of PHE290's participation in van der Waals interactions. These two residues, along with the aromatic peripheral site residues, make up the acyl binding pocket of TcAChE. They stabilize the attached ligands by establishing an aromatic continuity with TRP84, PHE330, and PHE331 of the hydrophobic patch. Our results were consistent with other studies, indicating that this aromatic network plays a key role in both inhibitor efficacy and substrate selectivity [51, 52].

All in all, the crystallographic ligand exhibited the highest binding affinity to TcAChE, forming the most extensive hydrogen bond network, engaging in PAS and the acyl pocket, but making no catalytic triad contact. Donepezil demonstrated its ability as a dual-site binder, interacting with both the PAS and catalytic site and having strong hydrophobic core interactions. These findings are consistent with its established clinical potency as a potent inhibitor of AChE. Kanzonol B also showed a high binding affinity to TcAChE, but slightly lower than that of donepezil and the crystallographic ligand. However, its interaction profile of PAS engagement, acyl pocket binding, and limited catalytic triad contact supports its possible role in inhibiting TcAChE activity. In view of this, kanzonol B can be considered for further investigation as a potential AChEI.

3.2. Drug likeness and ADMET studies

The amount of rotatable bonds explains strong intestinal availability, while MW, TPSA, and LogP suggest good membrane permeability and oral bioavailability [53]. The rule of five (RO5) [54] is another name for Lipinski's rule, which is used to determine if a chemical compound possesses characteristics that support its use as an oral medication. Lipinski's rule states that a molecule with a molecular weight greater than 500 Da, lipophilicity (LogP), hydrogen-bond donors (HBD) greater than 5, and hydrogen-bond acceptors greater than 10 is likely to have poor absorption or penetration [55, 56]. The requirements for bioavailability are further refined by Veber's rule (VR), which consists of two basic rules that compounds should follow for optimal bioavailability: TPSA \leq 140 Ų and rotatable bonds \leq 10 [57].

According to SwissADME, kanzonol B has a MW of 322.35, an iLogP of 3.10, three rotatable bonds, two donors, four hydrogen bond acceptors, and a TPSA of 66.76. The results of the drug-likeness predictions showed that it had good oral bioavailability and adhered to Veber's and Lipinski's rules [Reproduced from Ref. 21].

Data obtained from SwissADME [Reproduced from Ref. 21] and PreADMET showed a CNS permeability of -1.879 for kanzonol B. According to the interpretation of CNS permeability, substances with a logPS > -2 are thought to be able to enter the CNS, while those with a logPS < -3 are thought to be unable to do so. Because of its high CNS permeability and capacity to cross the blood-brain barrier, kanzonol B can potentially treat neurological illnesses by avoiding drug-hindering obstacles. Compounds having C_{brain}/C_{blood} values > 2.0

are easily able to pass through the blood–brain barrier (BBB). Compounds with blood/brain ratios between 2 and >0.1 have a moderate level of BBB penetration. On the other hand, substances with $C_{\text{brain}}/C_{\text{blood}}$ values less than 0.1 diffuse poorly into the brain [58]. Kanzonol B has a BBB ($C_{\text{brain}}/C_{\text{blood}}$) value between $2 > C_{\text{brain}}/C_{\text{blood}} > 0.1$, which indicates this compound has moderate absorption to the BBB. This BBB permeability is a crucial pharmaceutical aspect, as we are targeting neurodegenerative disease, and this compound should be able to cross the BBB for pharmaceutical action.

Kanzonol B is also predicted to have human intestinal absorption (HIA) of 93.89% and Caco2 cell permeability of 28.13 nm/sec, which suggests that it has middle permeability across Caco2 cells and is well absorbed after oral administration. Compounds with a bioavailability score (BA) of 0.55 or 0.56 are considered optimal and well absorbed by the body [59-61]. Kanzonol В has favorable pharmacokinetic characteristics with a BA score of 0.55 or 0.56 [Reproduced from Ref. 21]. Six isoenzymes, namely CYP1A2, CYP2C9, CYP2C19, CYP2D6, CYP2E1, and CYP3A4, carry out 90% of drug metabolism in the human body [62]. It is anticipated that CYP2C9, CYP1A2, CYP2C19, and CYP3A4 will play a role in kanzonol B metabolism. CYP3A4 and CYP2D6 are principally responsible for donepezil's metabolism, according to earlier research [63, 64]. As with the wellknown medication donepezil, kanzonol B was anticipated to have strong oral bioavailability, high GI absorption, and good absorbance in the human gut.

3.3. Boiled egg for GI absorption and brain penetration prediction

The BBB's permeability and GI absorption capacity are evaluated using the BOILED-egg model [65]. The yellow portion (yolk) in the BOILED-Egg model denotes a high likelihood of brain penetration, while the white region represents a high likelihood of passive absorption by the GI tract. Additionally, the spots are colored red if they are projected to be a non-substrate of P-gp (PGP-) and blue if they are predicted to be actively effluxed by P-gp (PGP+) [66].

The BOLIED-Egg models for kanzonol B and donepezil were within the prediction area. Both were found in the volk of a boiled egg, implying that these chemicals can passively diffuse over the BBB and generate minor CNS side effects [Reproduced from Ref. 21]. However, kanzonol B was anticipated not to be pumped out by p-glycoprotein (PGP) efflux (red dot), while donepezil was a PGP+ (blue dot), indicating that active efflux in the presence of PGP may reduce the intracellular drug concentration, decreasing therapeutic impact of donepezil. Besides, drugs that are PGP substrates usually show poor bioavailability due to low permeability [67]. Therefore, compared to donepezil, kanzonol B may offer improved therapeutic efficacy and bioavailability by avoiding PGP-mediated efflux, making it a potentially more effective candidate.

3.4. Toxicity prediction results

The kanzonol B was investigated for its toxicity using several toxicological endpoints, and its results are shown in Table 6.

Table 6. Toxicity profile of kanzonol B

Toxicity perspective category	Endpoint name	Endpoint unit	Prediction	Toxicity confidence	Prediction interpretation
	LD ₅₀ Score (mg/kg)*		3800		
	Toxicity Class*		5		
	Neurotoxicity*		Safe		
Nuclear Response	NR-AR**	Category (Toxic/Safe)	Safe	0.02	High Safety
Nuclear Response	NR-AR-LBD**	Category (Toxic/Safe)	Safe	0	High Safety
Nuclear Response	NR-AhR**	Category (Toxic/Safe)	Safe	0.3	Medium Safety
Nuclear Response	NR-Aromatase**	Category (Toxic/Safe)	Safe	0.08	High Safety
Nuclear Response	NR-ER**	Category (Toxic/Safe)	Toxic	0.52	Low Toxicity
Nuclear Response	NR-ER-LBD**	Category (Toxic/Safe)	Safe	0.12	High Safety
Nuclear Response	NR-PPAR-gamma**	Category (Toxic/Safe)	Safe	0.02	High Safety
Nuclear Response	NR-GR**	Category (Toxic/Safe)	Safe	0.31	Medium Safety
Nuclear Response	NR-TR**	Category (Toxic/Safe)	Safe	0.2	Medium Safety
Stress Response	SR-ARE**	Category (Toxic/Safe)	Safe	0.44	Low Safety
Stress Response	SR-ATAD5**	Category (Toxic/Safe)	Safe	0.06	High Safety
Stress Response	SR-HSE**	Category (Toxic/Safe)	Safe	0.29	Medium Safety
Stress Response	SR-MMP**	Category (Toxic/Safe)	Toxic	0.56	Low Toxicity
Stress Response	SR-p53**	Category (Toxic/Safe)	Toxic	0.51	Low Toxicity
Genomic	AMES Mutagenesis**	Category (Toxic/Safe)	Safe	0.33	Medium Safety
Genomic	Carcinogenesis**	Category (Toxic/Safe)	Safe	0.1	High Safety
Genomic	Micronucleus**	Category (Toxic/Safe)	Toxic	0.5	Low Toxicity
Environmental	Fathead Minnow**	Category (Toxic/Safe)	Toxic	0.99	High Toxicity
Environmental	T. Pyriformis**	Category (Toxic/Safe)	Toxic	0.99	High Toxicity
Environmental	Honey Bee**	Category (Toxic/Safe)	Safe	0.47	Low Safety
Environmental	Biodegradation**	Category (Toxic/Safe)	Safe	0.1	High Safety
Environmental	Crustacean**	Category (Toxic/Safe)	Toxic	0.74	Medium Toxicity
Environmental	Avian**	Category (Toxic/Safe)	Safe	0	High Safety
Environmental	Fathead Minnow (Regression)**	pLC50 [log(mg/L)]	-1	-	Toxicity is indicated when pLC50 < -0.3
Environmental	T. Pyriformis (Regression)**	pIGC50 [log (ug/L)]	-1	-	Toxicity is indicated when pIGC50 > -0.5
Environmental	Rat (Acute)**	LD50 [mol/kg]	-1	-	-
Environmental	Rat (Chronic Oral)**	LOAEL [log(mg/kg_bw/day)]	-1	-	-
Dose Response	Maximum Tolerated Dose**	MRTD [log(mg/kg/day)]	-1	-	Toxicity is indicated when MRTD > 0.477
Organic	Skin Sensitisation**	Category (Toxic/Safe)	Toxic	0.73	Medium Toxicity
Organic	hERG I Inhibitor**	Category (Toxic/Safe)	Safe	0.05	High Safety
Organic	hERG II Inhibitor**	Category (Toxic/Safe)	Safe	0.32	Medium Safety
Organic	Liver Injury I**	Category (Toxic/Safe)	Toxic	0.83	Medium Toxicity
Organic	Liver Injury II**	Category (Toxic/Safe)	Safe	0.21	Medium Safety

Toxicity perspective category	Endpoint name	Endpoint unit	Prediction	Toxicity confidence	Prediction interpretation
Organic	Eye Irritation**	Category (Toxic/Safe)	Safe	0.06	High Safety
Organic	Eye Corrosion**	Category (Toxic/Safe)	Safe	0	High Safety
Organic	Respiratory Disease**	Category (Toxic/Safe)	Safe	0.49	Low Safety

According to the toxicity prediction, kanzonol B is safe because it belongs to Class V (potentially dangerous if swallowed (2000 < LD50 \le 5000 in mg/kg)). Based on the toxCSM predictions, most of the nuclear receptor-related responses are considered safe, except NR-ER. Similarly, in the stress response category, most endpoints are predicted to be safe, except for SR-MMP and SR-p53, which exhibit low toxicity. Under the genomic category, kanzonol B is predicted to have low toxicity for the micronucleus endpoint. In terms of environmental toxicity, kanzonol B is predicted to be highly toxic to fathead minnows and Tetrahymena pyriformis and moderately toxic to crustaceans. For organic endpoints, most of them are safe, except for skin sensitization and liver injury, which have moderate toxicity. Notably, the hERG 1/II inhibition, associated with cardiotoxicity, shows no risk of toxicity, which is a favorable outcome. Overall, the majority of endpoints suggest that kanzonol B falls within the safe toxicity range.

4. Conclusions

In this work, we investigated the affinity of kanzonol B against TcAChE using molecular docking experiments. Kanzonol B demonstrated a significant binding affinity for the TcAChE active site, according to our molecular docking studies. The results indicated that it would be a successful AChEI. It has good bioavailability, GI absorption, CNS permeability, and BBB permeability, and it complies with Lipinski's and Veber's rules. Above all, it is regarded as safe for usage with toxicity class V. Kanzonol B is a potentially viable AChEI agent because of all these factors. Kanzonol B may have therapeutic potential for epilepsy because AChEIs have been shown to have neuroprotective and anticonvulsant properties. Nevertheless, additional experimental research and validations are necessary to validate its potential for clinical application.

Declaration of interest

The authors declare that they have no known competing financial interests or personal relationships that could have appeared to influence the work reported in this paper.

Acknowledgements

The authors are grateful to the Ministry of Education, Malaysia, for providing funds to the current research work under the fundamental research grant scheme [FRGS/1/2023/WAB13/AIMST/01/1]. Authors also extend their thanks to AIMST University for providing the necessary facilities to carry out the work.

References

- [1]. V.L. Feigin, T. Vos, E. Nichols, M.O. Owolabi, W.M. Carroll, M. Dichgans, G. Deuschl, P. Parmar, M. Brainin, C. Murray, The global burden of neurological disorders: translating evidence into policy, Lancet Neurology 19 (2020) 255–265. DOI: 10.1016/S1474-4422(19)30411-9
- [2]. Y.A. Ismail, Y. Haitham, M. Walid, H. Mohamed, Y.M.A. El-Satar, Efficacy of acetylcholinesterase inhibitors on reducing hippocampal atrophy rate: a systematic review and meta-analysis, BMC Neurology 25 (2025) 60. DOI: 10.1186/s12883-024-03933-4
- [3]. L. Fan, R. Wang, Q. Zan, K. Zhao, Y. Zhang, Y. Huang, X. Yu, Y. Yang, W. Lu, S. Shuang, X. Yang, C. Dong, A near-infrared fluorescent probe for visualization of acetylcholinesterase flux in the acute epileptic mice brain, Chemical and Biomedical Imaging 3 (2025) 332–340. DOI: 10.1021/cbmi.4c00058
- [4]. P. Li, S. Liu, Q. Liu, J. Shen, R. Yang, B. Jiang, C. He, P. Xiao, Screening of acetylcholinesterase inhibitors and characterizing of phytochemical constituents from *Dichocarpum auriculatum* (Franch.) W.T. Wang & P. K. Hsiao through UPLC-MS combined with an acetylcholinesterase inhibition assay in vitro, Journal of Ethnopharmacology 245 (2019) 112185. DOI: 10.1016/j.jep.2019.112185
- [5]. J. Xie, H. Jiang, Y.H. Wan, A.Y. Du, K.J. Guo, T. Liu, W.Y. Ye, X. Niu, J. Wu, X.Q. Dong, X.J. Zhang, Induction of a 55 kDa acetylcholinesterase protein during apoptosis and its negative regulation by the Akt pathway, Journal of Molecular Cell Biology 3 (2011) 250-259. DOI: 10.1093/jmcb/mjq047
- [6]. X.J. Zhang, D.S. Greenberg, Acetylcholinesterase Involvement in Apoptosis, Frontiers in Molecular Neuroscience 5 (2012) 40. DOI: 10.3389/fnmol.2012.00040
- [7]. L.E. Paraoanu, P.G. Layer, Acetylcholinesterase in cell adhesion, neurite growth and network formation, The FEBS Journal 275 (2008) 618–624. DOI: 10.1111/j.1742-4658.2007.06237.x
- [8]. S. Ruangritchankul, P. Chantharit, S. Srisuma, L.C. Gray, Adverse drug reactions of acetylcholinesterase inhibitors in older people living with dementia: a comprehensive literature review, Therapeutics and Clinical Risk Management 17 (2021) 927–949. DOI: 10.2147/TCRM.S323387
- [9]. E. Kröger, M. Mouls, M. Wilchesky, M. Berkers, P.-H. Carmichael, R. van Marum, P. Souverein, T. Egberts, M.L. Laroche, Adverse drug reactions reported with cholinesterase inhibitors: an analysis

- of 16 years of individual case safety reports from VigiBase, Annals of Pharmacotherapy 49 (2015) 1197–1206. DOI: 10.1177/1060028015602274
- [10]. C.C. Tan, J.T. Yu, H.F. Wang, M.S. Tan, X.F. Meng, C. Wang, T. Jiang, X.C. Zhu, L. Tan, Efficacy and safety of donepezil, galantamine, rivastigmine, and memantine for the treatment of Alzheimer's disease: a systematic review and meta-analysis, Journal of Alzheimers Disease JAD 41 (2014) 615–631. DOI: 10.3233/JAD-132690
- [11]. T.B. Ali, T.R. Schleret, B.M. Reilly, W.Y. Chen, R. Abagyan, Adverse effects of cholinesterase inhibitors in dementia, according to the pharmacovigilance databases of the United States and Canada, PLOS One 10 (2015) e0144337. DOI: 10.1371/journal.pone.0144337
- [12]. D.L. Bai, X.C. Tang, X.C. He, Huperzine A, a potential therapeutic agent for the treatment of Alzheimer's disease, Current Medicinal Chemistry 7 (2000) 355–374. DOI: 10.2174/0929867003375281
- [13]. R. Gersner, D. Ekstein, S.C. Dhamne, S.C. Schachter, A. Rotenberg, Huperzine a prophylaxis against pentylenetetrazole-induced seizures in rats is associated with increased cortical inhibition, Epilepsy Research 117 (2015) 97–103. DOI: 10.1016/j. eplepsyres.2015.08.012
- [14]. A. Mishra, R.K. Goel, Adjuvant anticholinesterase therapy for the management of epilepsy-induced memory deficit: a critical pre-clinical study, Basic Clinical Pharmacology Toxicology 115 (2014) 512–517. DOI: 10.1111/bcpt.12275
- [15]. E. Rębas, Role of flavonoids in protecting against neurodegenerative diseases possible mechanisms of action, International Journal of Molecular Science 26 (2025) 4763. DOI: 10.3390/ijms26104763
- [16]. T. Minocha, H. Birla, A.A. Obaid, V. Rai, P. Sushma, C. Shivamallu, M. Moustafa, M. Al-Shehri, A. Al-Emam, M.A. Tikhonova, S.K. Yadav, B. Poeggeler, D. Singh, S.K. Singh, Flavonoids as promising neuroprotectants and their therapeutic potential against Alzheimer's disease, Oxidative Medicine and Cellular Longevity 2022 (2022) 6038996. DOI: 10.1155/2022/6038996
- [17]. M. Ramezani, A.Z. Meymand, F. Khodagholi, H.M. Kamsorkh, E. Asadi, M. Noori, K. Rahimian, A.S. Shahrbabaki, A. Talebi, H. Parsaiyan, S. Shiravand, N. Darbandi, A role for flavonoids in the prevention and/or treatment of cognitive dysfunction, learning, and memory deficits: a review of preclinical and clinical studies, Nutritional Neuroscience 26 (2023) 156–172. DOI: 10.1080/1028415X.2022.2028058
- [18]. M.S. Uddin, M.T. Kabir, K. Niaz, P. Jeandet, C. Clément, B. Mathew, A. Rauf, K.R.R. Rengasamy, E. Sobarzo-Sánchez, G.M. Ashraf, L. Aleya, Molecular insight into the therapeutic promise of flavonoids against Alzheimer's disease, Molecules 25 (2020) 1267. DOI: 10.3390/molecules25061267

- [19]. T. Fukai, J. Nishizawa, T. Nomura, Five isoprenoid-substituted flavonoids from *Glycyrrhiza eurycarpa*, Phytochemistry 35 (1994) 515–519. DOI: 10.1016/S0031-9422(00)94793-9
- [20]. J.R. Fan, Y. Kuang, Z.Y. Dong, Y. Yi, Y.X. Zhou, B. Li, X. Qiao, M. Ye, Prenylated phenolic compounds from the aerial parts of *Glycyrrhiza* uralensis as PTP1B and α-glucosidase inhibitors, Journal of Natural Products 83 (2020) 814–824. DOI: 10.1021/acs.jnatprod.9b00262
- [21]. L.J. Siang, K. Vijeepallam, A. Muthuraman, P. Pavadai, T. Karunakaran, V. Ravichandran, Exploration of *Canarium odontophyllum* fruit phytoconstituents as potential candidates against epilepsy using in silico studies. Journal of Genetic Engineering and Biotechnology 23 (2025) 100561. DOI: 10.1016/j.jgeb.2025.100561
- [22]. D.H. Kim, H. Li, Y.E. Han, J.H. Jeong, H.J. Lee, J.H. Ryu, Modulation of inducible nitric oxide synthase expression in LPS-stimulated BV-2 microglia by prenylated chalcones from *Cullen corylifolium* (L.) Medik. through inhibition of I-κBα degradation, Molecules 23 (2018) 109. DOI: 10.3390/molecules23010109
- [23]. M.N. Arthur, K. Bebla, E. Broni, C. Ashley, M. Velazquez, X. Hua, R. Radhakrishnan, S.K. Kwofie, W.A. Miller, Design of inhibitors that target the Menin-Mixed-Lineage leukemia interaction, Computation 12 (2024) 3. DOI: 10.3390/computation12010003
- [24]. T.P. Saliu, H.I. Umar, O.J. Ogunsile, M.O. Okpara, N. Yanaka, O.O. Elekofehinti, Molecular docking and pharmacokinetic studies of phytocompounds from Nigerian Medicinal Plants as promising inhibitory agents against SARS-CoV-2 methyltransferase (nsp16), Journal of Genetic Engineering and Biotechnology 19 (202AD) 172. DOI: 10.1186/s43141-021-00273-5
- [25]. R. Veerasamy, R. Seenivasan, H. Rajak, P. Pavadai, P. Thangavelu, Mushroom-derived compounds unveiled naringin as a potential multi-targeted anti-breast cancer compound -an in-silico approach, Journal of Faculty of Pharmacy of Ankara University 49 (2025) 21–41. DOI: 10.33483/jfpau.1512113
- [26]. W.R. Mir, B.A. Bhat, M.A. Rather, S. Muzamil, A. Almilaibary, M. Alkhanani, M.A. Mir, Molecular docking analysis and evaluation of the antimicrobial properties of the constituents of *Geranium wallichianum* D. Don ex Sweet from Kashmir Himalaya, Scientific Report 12 (2022) 12547. DOI: 10.1038/s41598-022-16102-9
- [27]. R. Dharavath, M. Sarasija, K.N. Prathima, M. Ram Reddy, S. Panga, V. Thumma, D. Ashok, Microwave-assisted synthesis of (6-((1-(4-aminophenyl)-1*H*-1,2,3-triazol-4-yl)methoxy)substituted benzofuran-2-yl)(phenyl)methanones, evaluation of *in vitro* anticancer, antimicrobial activities and molecular docking on COVID-19, Results in Chemistry 4 (2022) 100628. DOI: 10.1016/j.rechem.2022.100628

- [28]. L. El Mchichi, A. El Aissouq, R. Kasmi, A. Belhassan, R. El-Mernissi, A. Ouammou, T. Lakhlifi, M. Bouachrine, *In silico* design of novel pyrazole derivatives containing thiourea skeleton as anti-cancer agents using: 3D QSAR, Drug-Likeness studies, ADMET prediction and molecular docking, Materials Today: Proceedings 45 (2021) 7661–7674. DOI: 10.1016/j.matpr.2021.03.152
- [29]. B. Asrar, N. Ali, I. Ali, M. Naveed, *In silico* investigation of ketamine and methylphenidate drug-drug conjugate for MDD and ADHD treatment using MD simulations and MMGBSA, Scientific Reports 15 (2025) 24565. DOI: 10.1038/s41598-024-82302-0
- [30]. N. Misuan, S. Mohamad, T. Tubiana, M.K.K. Yap, Ensemble-based molecular docking and spectrofluorometric analysis of interaction between cytotoxin and tumor necrosis factor receptor 1, Journal of Biomolecular Structure and Dynamics 41 (2023) 15339–15353. DOI: 10.1080/07391102.2023.2188945
- [31]. K. Petsri, M. Yokoya, S. Tungsukruthai, T. Rungrotmongkol, B. Nutho, C. Vinayanuwattikun, N. Saito, T. Matsubara, R. Sato, P. Chanvorachote, Structure—activity relationships and molecular docking analysis of Mcl-1 targeting renieramycin T analogues in patient-derived lung cancer cells, Cancers 12 (2020) 875. DOI: 10.3390/cancers12040875
- [32]. N.T. Tran, I. Jakovlić, W.M. Wang, In silico characterisation, homology modelling and structure-based functional annotation of blunt snout bream (*Megalobrama amblycephala*) Hsp70 and Hsc70 proteins, Journal of Animal Science and Technology 57 (2015) 44. DOI: 10.1186/s40781-015-0077-x
- [33]. C. Colovos, T.O. Yeates, Verification of protein structures: Patterns of nonbonded atomic interactions, Protein Science 2 (1993) 1511–1519. DOI: 10.1002/pro.5560020916
- [34]. A. Elengoe, M.A. Naser, S. Hamdan, Modeling and docking studies on novel mutants (K71L and T204V) of the ATPase domain of human heat shock 70 kDa protein 1, International Journal of Molecular Sciences 15 (2014) 6797–6814. DOI: 10.3390/ijms15046797
- [35]. R.A. Laskowski, M.W. MacArthur, D.S. Moss, J.M. Thornton, PROCHECK: a program to check the stereochemical quality of protein structures, Journal of Applied Crystallography 26 (1993) 283–291. DOI: 10.1107/S0021889892009944
- [36]. M. Wiederstein, M.J. Sippl, ProSA-web: interactive web service for the recognition of errors in three-dimensional structures of proteins, Nucleic Acids Research 35 (2007) W407–W410. DOI: 10.1093/nar/gkm290
- [37]. M. Mohanty, P.S. Mohanty, Molecular docking in organic, inorganic, and hybrid systems: a tutorial review, Monatshefte Chemistry 154 (2023) 683–707. DOI: 10.1007/s00706-023-03076-1
- [38]. M.R.F. Pratama, H. Poerwono, S. Siswodihardjo, Introducing a two-dimensional graph of docking

- score difference vs. similarity of ligand-receptor interactions, Indonesian Journal of Biotechnology 26 (2021) 54–60. DOI: 10.22146/ijbiotech.62194
- [39]. D. Ramírez, J. Caballero, Is it reliable to take the molecular docking top scoring position as the best solution without considering available structural data?, Molecules 23 (2018) 1038. DOI: 10.3390/molecules23051038
- [40]. M.J. Alves, H.J.C. Froufe, A.F.T. Costa, A.F. Santos, L.G. Oliveira, S.R.M. Osório, R.M.V. Abreu, M. Pintado, I.C.F.R. Ferreira, Docking studies in target proteins involved in antibacterial action mechanisms: extending the knowledge on standard antibiotics to antimicrobial mushroom compounds, Molecules 19 (2014) 1672–1684. DOI: 10.3390/molecules19021672
- [41]. D.R. Houston, M.D. Walkinshaw, Consensus docking: improving the reliability of docking in a virtual screening context, Journal of Chemical Information and Modeling 53 (2013) 384–390. DOI: 10.1021/ci300399w
- [42]. B. Divya, J. Narayanan, V. Chitra, T. Tamilanban, Evaluation of anti-convulsant activity of olivetol on PTZ-induced seizure model, Neuroquantology 20 (2022) 372–80.
- [43]. G. Ahmad, N. Rasool, K. Rizwan, I. Imran, A.F. Zahoor, M. Zubair, Synthesis, *in-vitro* cholinesterase inhibition, *in-vivo* anticonvulsant activity and *in-silico* exploration of *N*-(4-methylpyridin-2-yl)thiophene-2-carboxamide analogs, Bioorganic Chemistry 92 (2019) 103216.
- [44]. S. Bon, M. Vigny, J. Massoulié, Asymmetric and globular forms of acetylcholinesterase in mammals and birds, Proceedings of the National Academy of Sciences 76 (1979) 2546–2550. DOI: 10.1073/pnas.76.6.2546
- [45]. S. Abubakar, B.K. Khor, K.Y. Khaw, V. Murugaiyah, K.L. Chan, Cholinesterase inhibitory potential of *Dillenia suffruticosa* chemical constituents and protective effect against Aβ–induced toxicity in transgenic *Caenorhabditis elegans* model, Phytomedicine Plus 1 (2021) 100022. DOI: 10.1016/j.phyplu.2021.100022
- [46]. R.T. Feunaing, J.A. Gbaweng Yaya, J.N. Nyemb, N.I. Bassigue, H.L. Ketsemen, C. Henoumont, A.K. Kandeda, A. Venditti, S. Laurent, E. Talla, Antiradical and anti-acethylcholinesterase constituents from the methylene chloride extract of *Ganoderma applanatum* (Pers.) Pat (Ganodermataceae) and molecular docking study, Natural Product Research (2025) 1–13. DOI: 10.1080/14786419.2025.2491113
- [47]. V.B.S.C. Thunuguntla, C.S. B, K.K. B, B. Js, Screening and *in silico* analysis of *Hyptis suaveolens* metabolites for acetylcholinesterase inhibition, Asian Journal of Pharmaceutical and Clinical Research 9 (2016) 148–153.
- [48]. F. Ur-Rehman, M.F. Khan, I. Khan, R. Roohullah, Molecular interactions of an alkaloid euchrestifoline as a new acetylcholinesterase inhibitor, Bangladesh Journal of Pharmacology 8 (2013) 361–364.

- [49]. J.L. Sussman, M. Harel, F. Frolow, C. Oefner, A. Goldman, L. Toker, I. Silman, Atomic structure of acetylcholinesterase from *Torpedo californica*: a prototypic acetylcholine-binding protein, Science 253 (1991) 872–879. DOI: 10.1126/science.1678899
- [50]. L. Pezzementi, F. Nachon, A. Chatonnet, Evolution of acetylcholinesterase and butyrylcholinesterase in the vertebrates: an atypical butyrylcholinesterase from the *Medaka Oryzias* latipes, PLOS One 6 (2011) e17396. DOI: 10.1371/journal.pone.0017396
- [51]. C. Seniya, G.J. Khan, K. Uchadia, Identification of potential herbal inhibitor of acetylcholinesterase associated Alzheimer's disorders using molecular docking and molecular dynamics simulation, Biochemistry Research International 2014 (2014) 705451. DOI: 10.1155/2014/705451
- [52]. M. Bajda, A. Więckowska, M. Hebda, N. Guzior, C.A. Sotriffer, B. Malawska, Structure-based search for new inhibitors of cholinesterases, International Journal of Molecular Sciences 14 (2013) 5608. DOI: 10.3390/ijms14035608
- [53]. Z.Y. Ibrahim, Gideon Adamu Shallangwa, A. Uzairu, S.E. Abechi, Molecular docking, druglikeness and SwissADME evaluations of the interactions of 2'-substituted Triclosan derivatives with *Plasmodium falciparum* Enoyl-Acyl carrier protein reductase, Malaysian Journal of Pharmaceutical Sciences 20 (2022) 51–64. DOI: 10.21315/mjps2022.20.2.5
- [54]. C.A. Lipinski, Lead- and drug-like compounds: the rule-of-five revolution, Drug Discovery Today: Technologies 1 (2004) 337–341. DOI: 10.1016/j.ddtec.2004.11.007
- [55]. C.A. Lipinski, F. Lombardo, B.W. Dominy, P.J. Feeney, Experimental and computational approaches to estimate solubility and permeability in drug discovery and development settings1, Advanced Drug Delivery Reviews 46 (2001) 3–26. DOI: 10.1016/S0169-409X(00)00129-0
- [56]. M.P. Pollastri, Overview on the rule of five, Current Protocols in Pharmacology 49 (2010) 9.12.1-9.12.8.DOI: 10.1002/0471141755.ph0912s49
- [57]. D.F. Veber, S.R. Johnson, H.Y. Cheng, B.R. Smith, K.W. Ward, K.D. Kopple, Molecular properties that influence the oral bioavailability of drug candidates, Journal of Medicinal Chemistry 45 (2002) 2615–2623. DOI: 10.1021/jm020017n
- [58]. X. Ma, C. Chen, J. Yang, Predictive model of blood-brain barrier penetration of organic compounds, Acta Pharmacologica Sinica 26 (2005) 500–512. DOI: 10.1111/j.1745-7254.2005.00068.x

- [59]. S. Kunwittaya, C. Nantasenamat, L. Treeratanapiboon, A. Srisarin, C. Isarankura-Na-Ayudhya, V. Prachayasittikul, Influence of logBB cut-off on the prediction of blood-brain barrier permeability, Biomedical and Applied Technology Journal 1 (2013) 16-34.
- [60]. J. Bojarska, M. Remko, M. Breza, I.D. Madura, K. Kaczmarek, J. Zabrocki, W.M. Wolf, A supramolecular approach to structure-based design with a focus on synthons hierarchy in ornithine-derived ligands: Review, synthesis, experimental and in silico studies, Molecules 25 (2020) 1135. DOI: 10.3390/molecules25051135
- [61]. Y.C. Martin, A bioavailability score, Journal of Medicinal Chemistry 48 (2005) 3164–3170. DOI: 10.1021/jm0492002
- [62] E. Stavropoulou, G.G. Pircalabioru, E. Bezirtzoglou, The role of cytochromes P450 in infection, Frontiers in Immunology 9 (2018) 89. DOI: 10.3389/fimmu.2018.00089
- [63]. A. Coin, M.V. Pamio, C. Alexopoulos, S. Granziera, F. Groppa, G. de Rosa, A. Girardi, G. Sergi, E. Manzato, R. Padrini, Donepezil plasma concentrations, CYP2D6 and CYP3A4 phenotypes, and cognitive outcome in Alzheimer's disease, European Journal of Clinical Pharmacology 72 (2016)711–717. 10.1007/s00228-016-2033-1
- [64] P.J. Tiseo, S.L. Rogers, L.T. Friedhoff, Pharmacokinetic and pharmacodynamic profile of donepezil HCl following evening administration, British Journal of Clinical Pharmacology 46 (1998) 13–18. DOI: 10.1046/j.1365-2125.1998.0460s1013.x
- [65]. A. Daina, V. Zoete, A BOILED-Egg to predict gastrointestinal absorption and brain penetration of small molecules, ChemMedChem 11 (2016) 1117– 1121. DOI: 10.1002/cmdc.201600182
- [66] F. Zafar, A. Gupta, K. Thangavel, K. Khatana, A.A. Sani, A. Ghosal, P. Tandon, N. Nishat, Physicochemical and pharmacokinetic analysis of anacardic acid derivatives, ACS Omega 5 (2020) 6021–6030. DOI: 10.1021/acsomega.9b04398
- [67]. F. Darusman, T. Rusdiana, I. Sopyan, H. Rahma, M. Hanifa, Recent progress in pharmaceutical excipients as P-glycoprotein inhibitors for potential improvement of oral drug bioavailability: A comprehensive overview, Pharmacia 72 (2025) 1–16. DOI: 10.3897/pharmacia.72.e140734

Received: 01.09.2025 Received in revised form: 08.10.2025 Accepted: 10.10.2025